Experimental Verification of the Inhomogeneous Energy-Density Driven Instability

M. E. Koepke, W. E. Amatucci, J. J. Carroll III, and T. E. Sheridan
Department of Physics, West Virginia University, Morgantown, West Virginia 26506-6315
(Received 7 January 1994)

A category of oscillation identified with the inhomogeneous energy-density driven instability has been experimentally verified. This mode exploits the free energy available from shear in the $\mathbf{E}\times\mathbf{B}$ flow velocity. This shear is produced experimentally by applying different voltages to a segmented disk electrode located on axis at the end of a Q machine plasma column. As plasma conditions are varied between the two parameter regimes that, according to theory, correspond to the current-driven and shear-driven waves, the expected transition in mode characteristics is observed.

PACS numbers: 52.35.Fp, 52.35.Qz, 94.20.Bb, 94.30.Gm

In this Letter we experimentally verify the existence of a new branch of plasma oscillation driven by velocity shear. Ganguli, Lee, and Palmadesso [1,2] predicted the existence of this new branch, which is distinct from the well-known Kelvin-Helmholtz (KH) branch and is driven by inhomogeneity in the wave energy density. This inhomogeneity is caused by velocity shear. Subsequently, Ganguli *et al.* [3] and Ganguli and Palmadesso [4] extended their formalism to include magnetic-field-aligned current (FAC) and investigated the coupling between this new inhomogeneous energy-density driven (IEDD) instability and the current-driven electrostatic ion-cyclotron (CDEIC) instability [5]. It was shown that depending on the magnitude of the parameter $R\equiv k_y v_E/k_z v_d$, one of the instabilities may dominate in the plasma system, and consequently have the greater impact in important processes involving wave-particle interactions, such as transport and energization. Here, k_y, k_z, v_E, and v_d are wave vectors and flows across and along the ambient magnetic field, respectively. While it was found that the higher frequency modes ($\omega\approx\omega_{ci}$) may benefit from the coupling of parallel and transverse flows [3,4], the low-frequency modes ($\omega\ll\omega_{ci}$) are stabilized by transverse shear [6]. This latter conclusion has recently been the subject of intense research in fusion plasmas where shear in the cross-field flow appears to stabilize the low-frequency modes [7]. The configuration where inhomogeneous flows are present transverse to the ambient magnetic field is especially relevant to a number of space applications [8] where the wide range of inhomogeneity scale lengths existing in geospace permits this velocity-shear free energy to couple to a variety of naturally occurring plasma waves. These microinstabilities may have significant implications regarding mesoscale transport [9], and hence they are the subject of our experimental investigation. We experimentally verify that, for $R\geq 0.1$, IEDD waves exist with the theoretically predicted characteristics. We also verify that these waves differ sufficiently from CDEIC waves that a transition in mode characteristics can be identified and related to the magnitude of R.

Past Q-machine experiments [10,11] have reported significant changes in ion-cyclotron mode characteristics that were attributed to transverse electric fields present in the plasma. It was suggested that velocity shear may be responsible for these effects. The method we adopt is to investigate waves in the limit of $R=0$, CDEIC waves, and benchmark our experiments with previous investigations [12,13]. Then we experimentally make the transition to the IEDD regime, $R\geq 0.1$, to investigate waves in the limit of large R. Establishing that waves can be generated in both the CDEIC and IEDD regimes is the first time such an experimental verification has been made. The results reported here regarding the coupling of the CDEIC and IEDD modes may be useful to investigators dealing with the implications of velocity-shear-driven instabilities in space.

Experiments are performed in a single-ended Q machine [14] using a potassium plasma column (3-cm radius, 80-cm length) with the following parameters: density $n\approx 10^9$ cm^{-3}, ion and electron temperatures $T_i\approx T_e\approx 0.2$ eV, undisturbed plasma potential $V_{p0}\approx -2$ V, ion-electron mass ratio $m_i/m_e=7.15\times 10^4$, magnetic field $B=1.5$ kG, and neutral pressure (during the experiment) $P_n\approx 3\times 10^{-6}$ torr. Density and plasma potential are measured using Langmuir probes [15] and emissive probes, respectively. The presence of the probe can influence the instability threshold but has a negligible effect on the saturated-mode properties. A segmented disk electrode [16,17] is used to produce and control transverse, localized, dc electric fields (TLE) contained entirely within a FAC channel whose radius is defined by the overall radius of the disk, which is 1.0 cm, or approximately five ion gyroradii. The disk electrode is made of two coplanar, concentric circular segments that are heated to prevent surface contamination. The applied voltages, V_a and V_b, on the outer annular segment (0.6 cm $< r <$ 1.0 cm) and on the inner button segment ($r < 0.5$ cm), respectively, are set with independent power supplies. The FAC is produced by biasing the segments positively with respect to V_{p0} so that electrons are collected. As one would expect, it is possible to excite CDEIC waves by either segment alone if the field-aligned current to that segment is above the CDEIC threshold and the other segment is electrically floating. When the segments are biased simultaneously but unequally, a localized radi-

0031-9007/94/72(21)/3355(4)$06.00

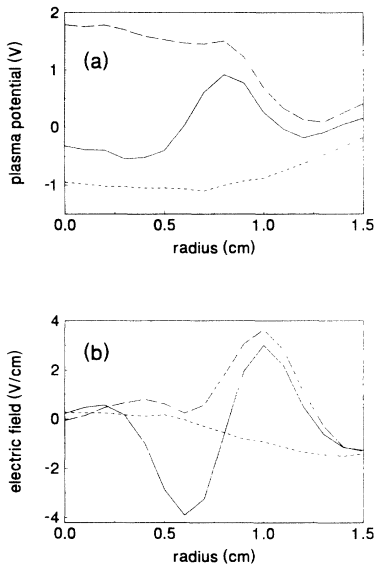

FIG. 1. Electrostatic profiles in the FAC channel ($r \leq 1.0$ cm): (a) potential and (b) electric field. Different lines correspond to the following (V_a, V_b) combinations: solid (20 V, 1 V), long-dashed (15 V, 15 V), and short-dashed (both disconnected). The solid line indicates the presence of the TLE entirely within the FAC channel. For this case, $E = -3.3$ V/cm would be used to calculate $v_E = E/B$ in the gap.

al electric field is produced within the FAC channel.

Doppler shifts are associated with the FAC-related axial drift velocity v_d (controlled primarily by $V_a + V_b$) and the TLE-related azimuthal $\mathbf{E}\times\mathbf{B}$ velocity v_E (controlled primarily by $\Delta V = V_a - V_b$). The parameter R ($\equiv k_\theta v_E / k_z v_d$, in cylindrical coordinates) is the ratio of the azimuthal and axial Doppler shifts and its value is the relevant parameter with which to follow the transition from one type of wave to the other [3]. For $R \ll 0.1$, the case of large v_d and small v_E, the waves are current driven. For $R \geq 0.1$, the case of smaller v_d and larger v_E, the waves are driven by the inhomogeneous dc electric field.

Figure 1 illustrates three radial profiles of the plasma potential $V_p(r)$ and the radial electric field, determined by $E_r = -dV_p/dr$. The short-dashed lines establish reference profiles. The long-dashed lines resemble unsegmented ("conventional") disk electrode behavior [13]. The solid lines demonstrate that a region of TLE can be created well inside the electron-current-channel boundary.

The value of v_E in the gap is determined using a two-gyroradii average of E_r that results in conservative (smaller) values of R if comparisons are made to theoretical predictions using the maximum of v_E in this TLE region. Gap values of $v_E/v_{te} = 0.012$, where v_{te} is the electron thermal speed, are typically obtainable. The minimum in the electric-field-gradient scale length $L_E = [(1/E)(\partial E/\partial r)]^{-1}$, the relevant transverse-velocity-shear scale length, occurs at gap radii and has a value approximately twice the ion gyroradius.

Two methods were used to measure v_d at radii associated with the gap. The segment method involves interpolating the current densities to the two disk electrode segments and using the density at gap radii to determine v_d. The probe method involves fitting the differentiated current-voltage characteristic of a translatable, directional (single-sided) Langmuir probe to a drifting-Maxwellian distribution function. Both methods yield similar results for v_d as a function of E_r, however, the segment method's results are adopted here because they have smaller uncertainty and because they are conservative (slightly larger) at larger values of E_r. Typical values of $v_d/v_{te} = 0.3$ are obtainable [17] at disk-electrode voltages of approximately 20 V. These values do not increase significantly for higher electrode voltages but they drop dramatically as the electrode voltage approaches the plasma potential, according to the electrode's current-voltage characteristic.

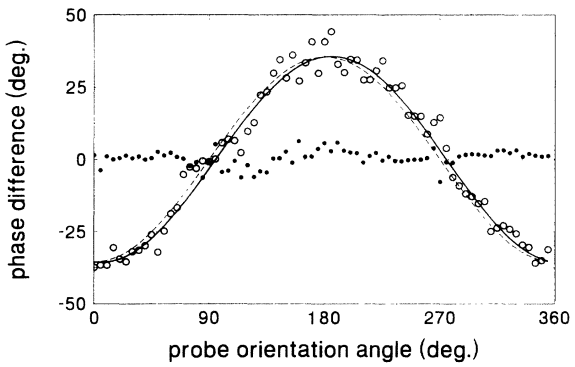

FIG. 2. Relative phase difference between tips of a two-probe array ($r_p = 0.55$ cm, 3-mm probe separation) as a function of the orientation between the vector connecting the two tips and the azimuthal unit vector. Open and closed circles are associated with IEDD and CDEIC fluctuations, respectively. Solid line is least-squares sinusoid calculated using the circles. Finite k_z is indicated by the deviation of the solid line from the dashed line associated with $k_z = 0$ and $k_\theta = 1.8$ cm^{-1}.

The measurement of k_θ and k_z involve the cross correlation of simultaneously acquired ion-saturation current fluctuations from two separated Langmuir probes mounted together and inserted radially into the plasma column to a point where the amplitude of each mode is large. To minimize contributions from radial phase behavior, the tips are placed at identical radii r_p. Rotating the probe shaft rotates the vector that connects the probe tips of such a two-probe array with respect to the azimuthal unit vector, and thus the azimuthal and axial separations ($\Delta\theta$ and Δz) of the probe tips ($r_p = 0.55$ cm, 3-mm probe separation) are varied through positive and negative maxima and zero. Alias azimuthal mode numbers are eliminated by highly resolving such a range of azimuthal separations. For traveling waves, $k_\theta = \Delta\phi/r_p\Delta\theta$ and $k_z = \Delta\phi/\Delta z$, where $\Delta\phi$ is the measured phase difference (in radians) between probe signals. From the values of $\Delta\phi$ in Fig. 2, k_θ for the CDEIC and IEDD fluctuations are determined to be zero ($k_\theta\rho_i < 10^{-4}$) and 1.8 cm^{-1} ($k_\theta\rho_i \approx 0.4$), re-

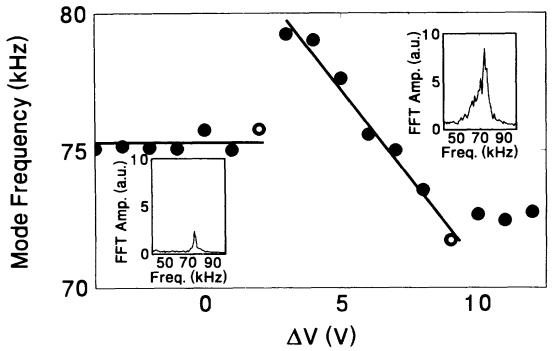

FIG. 3. Behavior of the mode frequency detected on annulus disk segment. Inset spectra, each corresponding to the nearer open-circle case, emphasize differences in CDEIC (left FFT) and IEDD-like (right FFT) modes. Each spectrum is an average of eight FFT's (each FFT is associated with a 1-mega-sample/sec time series with 1024 points).

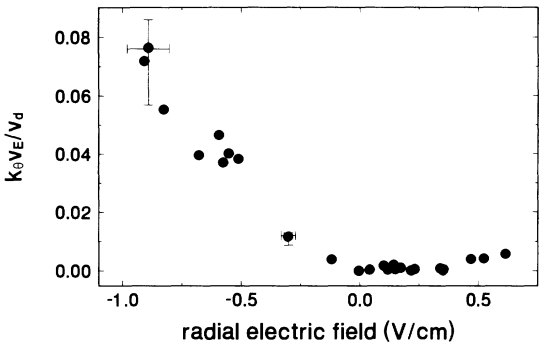

FIG. 4. Dependence of $K \equiv k_\theta v_E / v_d$ (in units of cm^{-1}) on transverse electric field.

spectively. Sinusoids calculated from a least-squares fit to $\Delta\phi$ indicate k_z values of 0.06 ± 0.06 cm^{-1} and 0.17 ± 0.11 cm^{-1} for the CDEIC and IEDD fluctuations, respectively. One such sinusoid (solid line) associated with the IEDD waves and a reference sinusoid (expected if k_z were zero and $k_\theta = 1.8$ cm^{-1}) are shown in Fig. 2. The open circles agree better with the nonzero-k_z line than with the zero-k_z line within experimental uncertainty. Note that the Kelvin-Helmholtz instability is associated with values of $k_z/k_\theta \ll 0.01$ [2] as well as $\omega \ll \omega_{ci}$.

Although the mode spectrum is not one of the quantities that determine the value of R, it readily distinguishes CDEIC and IEDD waves. To identify a region of (V_a, V_b) parameter space containing the two types of waves that is suitable for demonstrating a transition in the value of R, the applied segment-voltage difference ΔV was varied until a transition in the mode spectrum was observed in the fluctuations in the current collected by the segments. Such a transition is evident at $\Delta V = 2.5$ V in Fig. 3 which shows the mode frequency for a sequence of ΔV values. At small values of ΔV in Fig. 3, the case $V_a \approx V_b \gg V_{p0}$ exists and enough FAC is present to excite CDEIC waves. At large values of ΔV in Fig. 3, the case $V_a \gg V_b > V_{p0}$ exists and sufficiently large shear excites IEDD-like waves at lower values of FAC subcritical to the CDEIC instability [18]. As expected, the CDEIC fluctuations have a frequency around $\omega \approx 1.2\omega_{ci}$, relatively independent of the magnitude of the TLE and the FAC [5]. Although the shear-driven mode frequency is also in the vicinity of the ion-cyclotron frequency, it shifts linearly with the segment-voltage difference ΔV, unlike the CDEIC mode frequency. Since ΔV is approximately proportional to the TLE in the plasma, this shift is consistent with the Doppler shift predicted for IEDD fluctuations [2,3]. Beyond $\Delta V = 10$ V, the frequency does not change because E_r in the plasma saturates [17]. Spectra corresponding to the two modes are shown as insets in Fig. 3 to emphasize the differences between the line shapes, single peaked and narrow band (FWHM ≈ 2.5 kHz, or 3%) for CDEIC waves and spiky and broad band (FWHM ≈ 12 kHz, or 16%) for IEDD waves, consistent with the simulations of Nishikawa *et al.* [19]. Frequencies below the potassium-cyclotron frequency are occasionally seen for these IEDD waves. Unlike the CDEIC mode amplitude which is independent of ΔV, the IEDD mode amplitude varies with ΔV. The maximum-amplitude condition may correspond to an optimum match between the mode's preferred structure, which theoretically depends on the magnitude of TLE, and the geometric constraints in the laboratory. The relative areas under the spectra in Fig. 3 indicate that for this value of ΔV the IEDD fluctuations are significantly larger than CDEIC fluctuations.

Data necessary to determine $K \equiv k_\theta v_E / v_d$ and identify the waves were acquired in a region of (V_a, V_b) parameter space in which both CDEIC and IEDD waves are included. These data were acquired at radii associated with the gap between disk-electrode segments, where, for the IEDD case, the TLE and the mode amplitude are largest, and for the CDEIC case, the mode amplitude is also large. Figure 4 displays the experimental transition of K from zero (the CDEIC regime) to approximately 0.08 cm^{-1} (well into the IEDD regime, i.e., $R \approx 0.5$) as the electric field in the plasma is increased. Larger values of K (e.g., $K = 0.3 \pm 0.1$ cm^{-1} and $R \approx 2$) can be consistently reached during experimental runs that concentrate exclusively on large-K conditions.

For cases in which **E** is directed radially outward (i.e., E is positive), $R = 0$ and CDEIC waves are observed. This is attributed to the fact that, for the fixed value of $V_a = 14$ V in Fig. 4, the FAC remains supercritical to the CDEIC instability for positive E (i.e., $V_b > V_a$). The fact that the FAC is larger for cases in which $V_b > V_a$ than for cases in which $V_b < V_a$ [20] is consistent with this observation. Another factor is the larger value of L_E (five-fold increase is typical) associated with the cases in which $V_a < V_b$, indicating reduced shear in v_E.

Distinguishing aspects of the radial and azimuthal mode structure are summarized in Fig. 5, which is a three-dimensional plot of the phase difference between

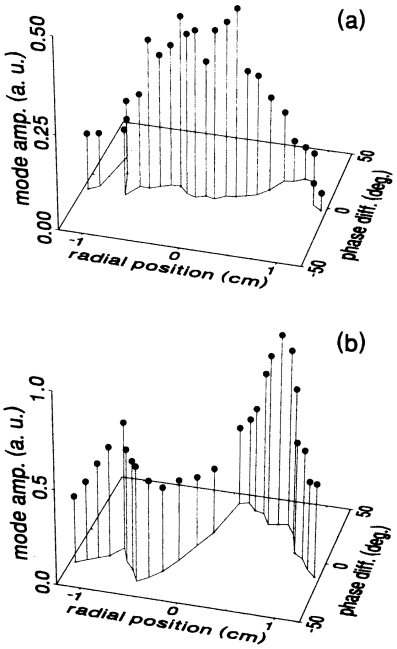

FIG. 5. Pin plot of mode amplitude and relative phase vs radius. (V_a, V_b) combinations are (a) (40 V, 40 V), CDEIC waves present, and (b) (14 V, −6 V), IEDD waves present. Probes are separated by 3 mm. Location of disk-electrode segments are indicated along position axis. Note that, in (b), amplitude maximum is located off-axis where shear is maximum.

signals from two azimuthally separated probes as a function of radius, with mode amplitude on the third axis. The current-driven case ($R=0$) shown in Fig. 5(a) is characterized by an on-axis maximum in mode amplitude and negligible phase shift—features consistent with previously reported investigations [13]. In contrast, the shear-driven case ($R \geq 0.1$) shown in Fig. 5(b) is characterized by an off-axis peak in mode amplitude in the region of largest shear in the transverse velocity. The nonzero values of phase difference, which reverse sign on opposite sides of the origin, indicate azimuthal propagation. This mode structure is consistent with the cylindrical analog of slab-model predictions [3].

In summary, these results establish that waves in both the CDEIC and IEDD regimes can be generated in the West Virginia University Q machine. The results reported here experimentally verify the IEDD instability which adds important support to the modeling and interpretation of *in situ* space data using theoretically predicted shear-driven instabilities [20,21].

We gratefully acknowledge numerous useful discussions with Dr. G. Ganguli on the theoretical aspects of the IEDD instability as well as his critical reading of this manuscript. We also gratefully acknowledge discussions and experimental assistance from Dr. M. J. Alport during his sabbatical visit at WVU. This research is supported by the ONR and the NSF.

[1] G. Ganguli, Y. C. Lee, and P. Palmadesso, Phys. Fluids **28**, 761 (1985).
[2] G. Ganguli, Y. C. Lee, and P. J. Palmadesso, Phys. Fluids **31**, 823 (1988).
[3] G. Ganguli, Y. C. Lee, P. J. Palmadesso, and S. L. Ossakow, in *Physics of Space Plasmas (1988)*, edited by T. Chang, G. B. Crew, and J. R. Jasperse (Scientific Publishers, Cambridge, MA, 1989), p. 231.
[4] G. Ganguli and P. J. Palmadesso, Geophys. Res. Lett. **15**, 103 (1988).
[5] W. E. Drummond and M. N. Rosenbluth, Phys. Fluids **5**, 633 (1962).
[6] G. Ganguli, Y. C. Lee, P. J. Palmadesso, and S. L. Ossakow, Geophys. Res. Lett. **16**, 735 (1989).
[7] B. Basu and B. Coppi, Phys. Fluids B **4**, 2817 (1992); J. Chen, R. G. Greaves, and A. K. Sen, Bull. Am. Phys. Soc. **36**, 2281 (1991).
[8] G. D. Earle, G. Ganguli, and M. C. Kelley, J. Geophys. Res. **94**, 15321 (1989); R. T. Tsunoda, R. C. Livingston, J. F. Vickery, R. A. Heelis, W. B. Hanson, F. J. Rich, and P. F. Bythrow, J. Geophys. Res. **94**, 15277 (1989); F. S. Mozer, C. W. Carlson, M. K. Hudson, R. B. Torbet, B. Paraday, J. Yatteau, and M. C. Kelley, Phys. Rev. Lett. **38**, 292 (1977).
[9] S. B. Ganguli and P. J. Palmadesso, J. Geophys. Res. **92**, 8673 (1987); R. L. Lysak, in *Ion Acceleration in the Magnetosphere and Ionosphere*, edited by T. Chang, AGU Monograph No. 38 (American Geophysical Union, Washington, DC, 1986), p. 261.
[10] M. Nakamura R. Hatakeyama, and N. Sato, in *Proceedings of the Second Symposium on Plasma Double Layers,* edited by R. Schrittwieser and G. Eder (University of Innsbruck, Innsbruck, 1984), p. 171; N. Sato, M. Nakamura, and R. Hatakeyama, Phys. Rev. Lett. **57**, 1227 (1986).
[11] E. G. van Niekerk, P. H. Krumm, and M. J. Alport, Plasma Phys. Controlled Fusion **33**, 375 (1991).
[12] R. W. Motley and N. D'Angelo, Phys. Fluids **6**, 296 (1963).
[13] J. J. Rasmussen and R. W. Schrittwieser, IEEE Trans. Plasma Sci. **19**, 457 (1991).
[14] N. Rynn and N. D'Angelo, Rev. Sci. Instrum. **31**, 1326 (1960).
[15] W. E. Amatucci, M. E. Koepke, T. E. Sheridan, M. J. Alport, and J. J. Carroll III, Rev. Sci. Instrum. **64**, 1253 (1993).
[16] M. E. Keopke and W. E. Amatucci, IEEE Trans. Plasma Sci. **20**, 631 (1992).
[17] J. J. Carroll III, M. E. Koepke, W. E. Amatucci, T. E. Sheridan, and M. J. Alport, Rev. Sci. Instrum. (to be published).
[18] W. E. Amatucci, M. E. Koepke, J. J. Carroll III, and T. E. Sheridan, Geophys. Res. Lett. (to be published).
[19] K.-I. Nishikawa, G. Ganguli, Y. C. Lee, and P. J. Palmadesso, Phys. Fluids **31**, 1568 (1988); J. Geophys. Res. **95**, 1029 (1990).
[20] G. Ganguli, M. J. Keskinen, H. Romero, R. Heelis, T. Moore, and C. Pollock, J. Geophys. Res. **99**, 8873 (1994).
[21] H. Romero, G. Ganguli, P. B. Dusenbery, and P. J. Palmadesso, Geophys. Res. Lett. **17**, 2313 (1990).